Colloid and Polymer Science (2018) 296:1927–1934
https://doi.org/10.1007/s00396-018-4419-3

ORIGINAL CONTRIBUTION

Polaron localization in polyaniline through methylene blue dye interaction for tuned charge transport and optical properties

Kamanashis Sarkar[1,2] · Krishna Deb[1] · Ajit Debnath[1] · Arun Bera[1] · Animesh Debnath[3] · Biswajit Saha[1]

Received: 24 May 2018 / Revised: 25 September 2018 / Accepted: 14 October 2018 / Published online: 24 October 2018
© Springer-Verlag GmbH Germany, part of Springer Nature 2018

Abstract

An excellent control over the charged transport process and optical properties in polyaniline has been attained through successful localization of polarons formed in the polyaniline chain. The localization of polaron in polyaniline has been achieved through its interaction with methylene blue (MB) dye. Polyaniline has been synthesized on paper substrate from aniline using $FeCl_3$ as polymerizing agent. On optical measurement of prepared sample, a remarkable red shift in the optical band gap has been observed varying from 2.63 to 2.47 eV. The charge transport behavior as reflected from its *I-V* measurement shows a nice tuning in the logarithmic scale. The chemical interaction between the MB dye and the polaronic charged defect states brings this brilliant tuning in the optical and electrical properties of polyaniline. Predominantly, the intra-chain charge transport of the polyaniline backbone is affected by the MB dye interaction.

Keywords Conjugated polymer · Optical properties · Electronic properties · Dye interaction

Introduction

The fundamental understanding of intra-chain and inter-chain charge transfer processes in conjugated polymers opened up an inspiring area of research nowadays. The electronic structure of π-conjugated molecules is of specific interest to scientists and researchers, particularly in semiconductor science and technology, in order to bring a tuning and alignment of energy levels to control the optical, electrical, and chemical catalytic properties [1–4]. In addition, the extensive delocalization and localization of defect states in the polymer chain provide outstanding opportunities in tuning their optical and electrical properties [5]. Thus, such π-conjugated molecules have been appearing with excellent physical properties, and as a result, conducting polymers such as polyaniline [6–8], polypyrrole [9, 10], polythiophene [11], and their derivatives have been widely investigated for application in electronic devices such as light-emitting diodes [12–14], solar cells [15–17], energy storage devices [18–20], catalytic applications [21, 22], thermoelectric devices [23–25], supercapacitors [26–29], and sensors [30–33] as active materials. Among different π-conjugated molecules, polyaniline is one with excellent physical properties and suitable electronic band structures [34], providing its possibility to be employed in electronic devices [35–39]. Moreover, polyaniline has advantages of its simpler polymerization process, low cost, and tunability of physical properties like electrical and optical properties [40–43].

Dye molecules are of special significance for their optical absorption properties, and they have chromophore for generating color in organic compounds. The chromophores are part of a conjugate system and thus likely to interact with π-conjugated molecules. Based on the fact that the partially oxidized polyaniline has positive charged defect states [44, 45], we approached to investigate the interaction of a dye with polyaniline. In this work, an attempt has been taken to observe the effect of methylene blue (MB) dye interaction with polyaniline, in tuning its optical and electrical properties. Especially, this polyaniline dye interaction has been observed on cellulose system, considering the advantages of flexibility and high hydrophilicity of cellulose, which provides

✉ Biswajit Saha
biswajit.physics@gmail.com

[1] Department of Physics, National Institute of Technology Agartala, Jirania, West Tripura 799046, India

[2] Department of Electronics and Communication Engineering, National Institute of Technology Agartala, Jirania, West Tripura 799046, India

[3] Department of Civil Engineering, National Institute of Technology Agartala, Jirania, West Tripura 799046, India

opportunities of better chemical interaction with dye solution and also during synthesis.

With the recent rapid progress of functionality of polymer-based electronic materials, one can also observe parallel developments in their synthesis techniques, which included a number of polymerization processes such as photo-induced polymerization [46, 47], interfacial polymerization [48, 49], electrochemical polymerization [50–52], solution polymerization [53, 54], seeding polymerization [55], emulsion polymerization [56], vapor phase self-assembling polymerization [57, 58], plasma polymerization [59, 60], and sonochemical synthesis process [61, 62] techniques. Considering the point of better control and uniformity over cellulose substrate, the vapor phase polymerization process has been chosen and employed for polyaniline synthesis in this article. Here, polymerization of aniline has been carried out using $FeCl_3$ as polymerizing agent. Subsequently, the polyaniline-coated cellulose sheet was used for MB dye interaction. The prepared MB dye–implanted polyaniline samples have been studied for structural analysis, optical properties, and electrical properties. A remarkable tuning has been achieved in the electrical transport properties along with optical properties, thus opening a wider and simpler way of functionalizing π-conjugated molecules on cellulose as an electronic material system.

Experimental details

Materials

Highly purified aniline, methanol, anhydrous ferric chloride (Merck), and methylene blue (Sigma-Aldrich) were used in the chemical synthesis process. Cellulose papers of thickness of 127 μm were used as the flexible substrates.

Synthesis of dye-implanted polyaniline on cellulose

Polymerization of aniline on cellulose was carried out from double-distilled aniline through vapor phase polymerization technique as detailed in our earlier report [63]. Partially oxidized emeraldine salt form of polyaniline has been obtained through this process using $FeCl_3$ as polymerizing agent. The prepared polyaniline-implanted cellulose sheets were then used for MB dye interaction. For that, powdered MB dye was dissolved in distilled water to prepare solutions of MB dye at four different concentrations of 1 mg/l, 3 mg/l, 7 mg/l, and 11 mg/l in four different beakers. Then, four pieces of polyaniline-implanted cellulose sheets were emerged into those beakers for desired interactions with MB dye at four different concentrations. All the samples were taken out from the dye solution and were dried on air at ambient temperature. The dye-interacted polyaniline-implanted cellulose sheets were thus produced and then used for different physical characterizations to study their functionality as electronic materials.

Characterizations

The prepared samples were studied for their physical properties through different characterization techniques. X-ray diffraction (XRD) measurements have been done to analyze crystal structure using XRD (Bruker D-8 Advance) system. Field emission scanning electron microscopy (FESEM) has been performed using JEOL (JSM-7200F) model for its morphological investigations. The optical absorbance has been measured by UV-Vis-NIR spectrophotometer (Shimadzu 3600 plus). The electrical properties were studied by electrical conductivity (*I-V*) measurements using Agilent (B2912A, USA) precision source/measurement.

Results and discussion

Structural and morphological characterizations

The crystal structure of the polyaniline-loaded cellulose has been investigated for both the cases before and after MB dye incorporation. The X-ray diffraction pattern has been depicted in Fig. 1, which shows one prominent peak appeared at $2\theta = 22.4^\circ$ and two small peaks at $2\theta = 38^\circ$ and $2\theta = 44.26^\circ$ corresponding to the Miller planes (020), (300), and (222) of polyaniline [5].

The X-ray diffraction measurements show that the degree of crystallinity of the polyaniline-loaded paper does not decline significantly due to MB dye interaction. The XRD peaks

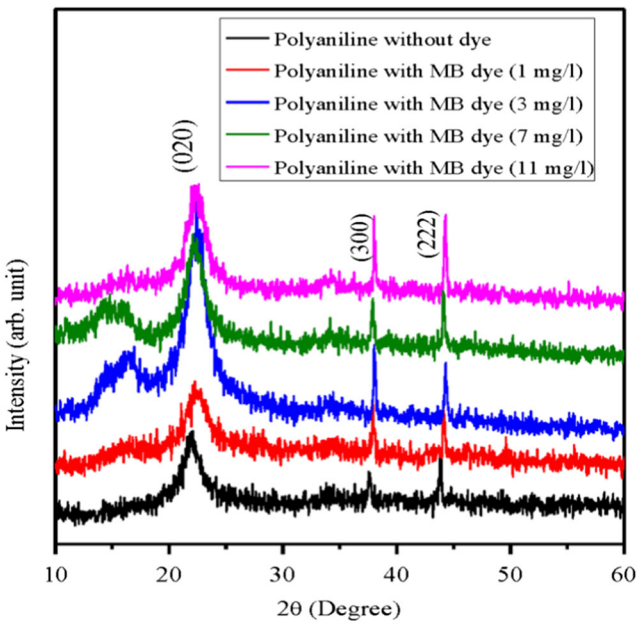

Fig. 1 X-ray diffraction pattern of dye-interacted polyaniline on cellulose

also indicate that the emeraldine salt form of polyaniline has been obtained during polymerization process, as intended during its synthesis process. The basic oxidation state of the polyaniline remains unaltered during dye interaction without further oxidation or reduction of the polymer chain by the interaction of MB dye.

Morphological and compositional analyses

The morphological investigation of the prepared polyaniline-coated cellulose has been done from field emission scanning electron microscopy (FESEM) measurements. Figure 2a represents the FESEM image of the polyaniline-implanted cellulose.

The FESEM image clearly depicts that the polyaniline has been successfully implanted over the cellulose sheet with excellent uniformity. In order to investigate the incorporation of MB dye on cellulose sheet, the FESEM image has been taken after dye loading as well, which is shown in Fig. 2b. This demonstrates uniform distribution of the loaded dye over the cellulose sheet. Further, the compositional analysis was performed from energy dispersive X-ray (EDX) measurement, in order to confirm the incorporation of MB dye. The EDX spectra of polyaniline-implanted cellulose with MB dye incorporation are shown in Fig. 3. The elemental detection by EDX measurements confirms the presence of MB dye over the polyaniline-implanted cellulose. In the EDX spectra, the presence of S, Cl, C, N, and O has been observed. Among these elements, C and N have appeared for both the compounds polyaniline and MB dye. But S and Cl have been observed due to the presence of MB dye only, since no other sources of S and Cl were used. Further, the UV-vis-NIR spectra (Fig. 4) of the dye-loaded polyaniline show the characteristic optical absorption of MB dye confirming the presence of MB dyes.

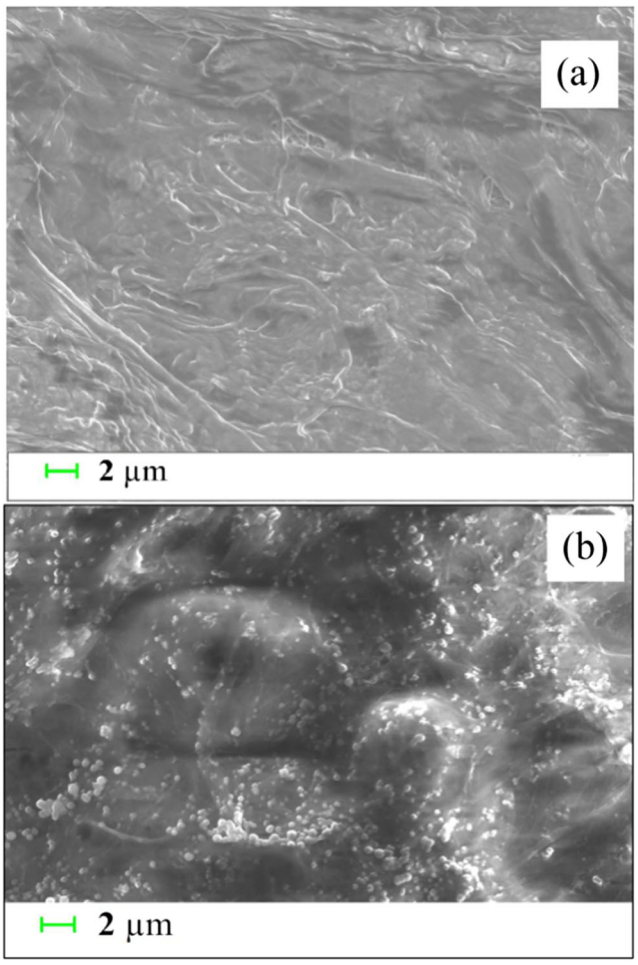

Fig. 2 **a** FESEM image of the polyaniline-implanted cellulose. **b** FESEM image taken after dye loading

Optical absorption spectroscopy

The interaction of organic π-conjugated molecules with electromagnetic radiation provides a convincing tool to investigate the energy band structure of such macromolecular systems. In order to understand the effect of MB dye on the fundamental optical absorption properties of polyaniline, optical absorption spectroscopic measurements have been done for polyaniline-implanted cellulose sheets interacted for different times with MB dye. The optical absorption spectra of polyaniline interacted with MB dye at 1 mg/l concentration are demonstrated in Fig. 4.

For the pure polyaniline, the absorption bands are centered at 255 nm, 355 nm, 400 nm, and 780 nm respectively. The absorption bands are due to the characteristic optical transitions of the emeraldine form of polyaniline. The weak peak appearing at 255 nm is related to the molecule conjugation [64]. The broad peak centered at 355 nm is due to π-π* transition within the benzenoid segments [65]. The absorption peak at 400 nm corresponds to polaron–π* transition and is related to doping level and formation of polaron [66]. Another broad characteristic absorption peak of polyaniline appearing at 780 nm attributes for π–polaron transition [65]. The MB dye has its characteristic absorptions occurring at 605 nm and 668 nm [67]. This fundamental absorption of MB dye occurs due to vibronic transitions and π-π* transitions.

The effect of MB dye treatment on the optical band gap of polyaniline has also been studied from optical absorption measurements. The optical band gap has been calculated from the fundamental relationship between the optical absorption coefficient (α) and the incident photon energy ($h\nu$) as given below

$$(\alpha h\nu)^{\frac{1}{n}} = A\left(h\nu - E_g\right) \quad (1)$$

where α, ν, E_g, and A denote the absorption coefficient, linear frequency of the incident photon, energy band gap, and an energy-independent constant, respectively. The

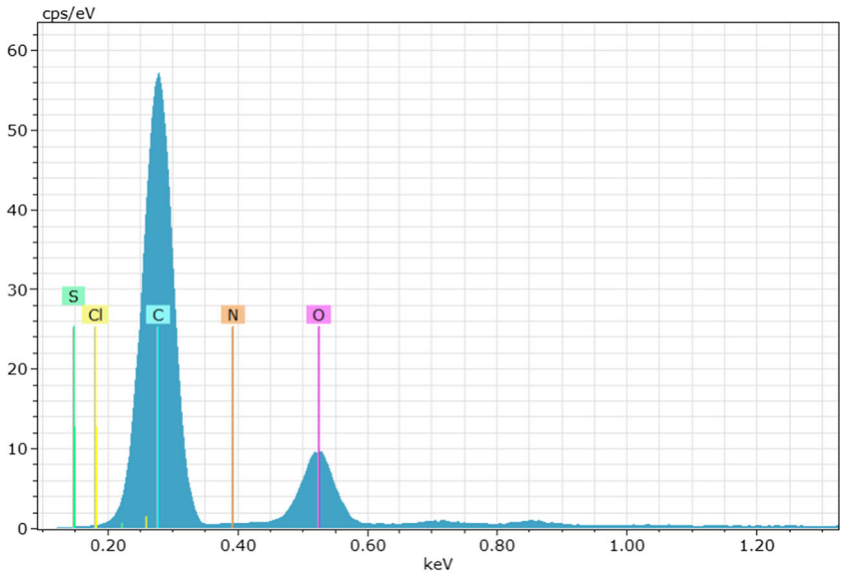

Fig. 3 The EDX spectra of the dye-loaded polyaniline-implanted cellulose

index n is related to the different types of transition. $n = \frac{1}{2}$ for a direct band allowed transition energy gap, $n = 2$ for an indirect allowed transition, $n = \frac{3}{2}$ for forbidden direct transition, and $n = 3$ for forbidden indirect transition energy gap. The optical energy band gap is obtained from the $(\alpha h\nu)^2$ vs. $(h\nu)$ plot by extrapolating the linear portion of the plot to the $(h\nu)$ axis, as illustrated in Fig. 5.

It has been observed that the energy band gap of polyaniline suffers a red shift during interaction with MB dye. Some inter-band defect levels have been created in the polyaniline band structure due to MB dye interaction, and this causes the decrease in energy band gap of polyaniline. This is also responsible for localizations of carriers affecting the electrical behavior of polyaniline interacted with MB dye, discussed in the next section.

Electrical properties

The polyaniline as prepared on cellulose shows electrical conductivity, and the charge transport process of the polyaniline-implanted cellulose is based on the formation of polaron and bipolaron charged defect states on the polymer backbone [63]. The overall electrical transport of polyaniline depends on the performance of two different transport processes, generally involved in such polymeric systems: intra-chain and inter-chain transport processes. The intra-chain charge transport is based on the delocalization of the carriers on the polymer chain and the effective conjugation length [68]. The inter-chain charge transport in polymeric system is based on the hopping mechanism, which is dependent on the ordered molecular packing. In

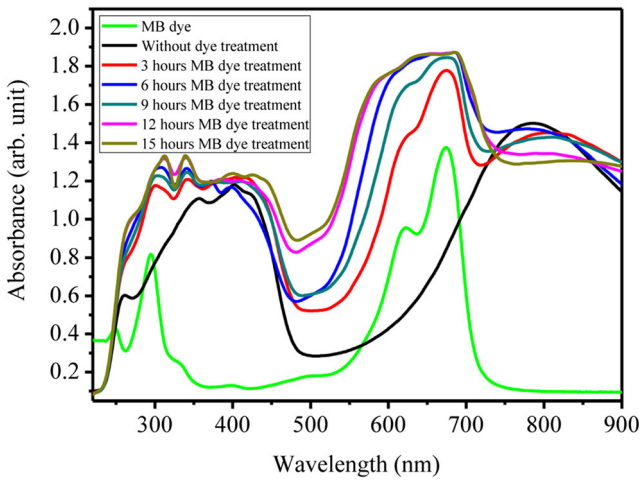

Fig. 4 Optical absorbance spectra of MB dye–interacted polyaniline on cellulose

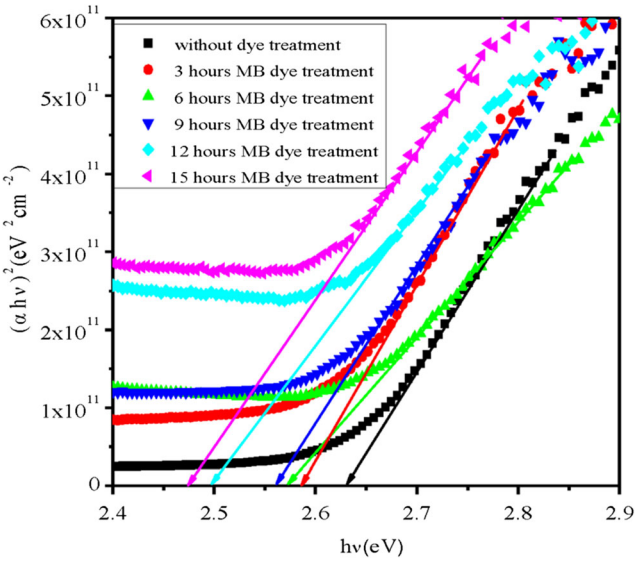

Fig. 5 Variation of optical band gap of polyaniline interacted with MB dye for different interaction times

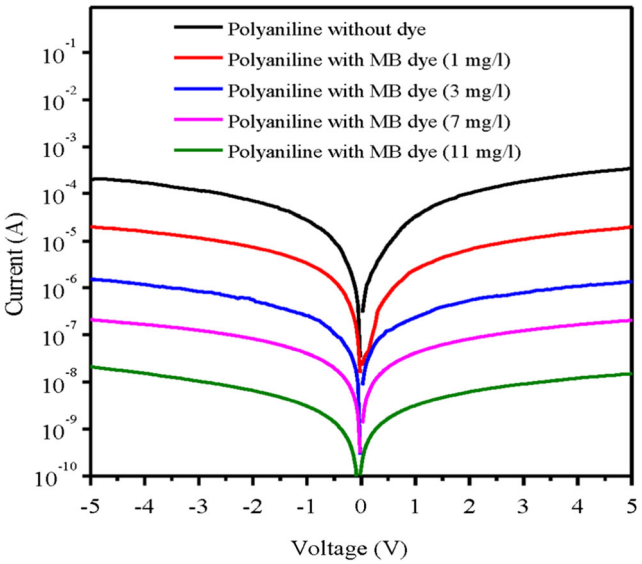

Fig. 6 Current vs. voltage plot of MB dye–interacted polyaniline on cellulose

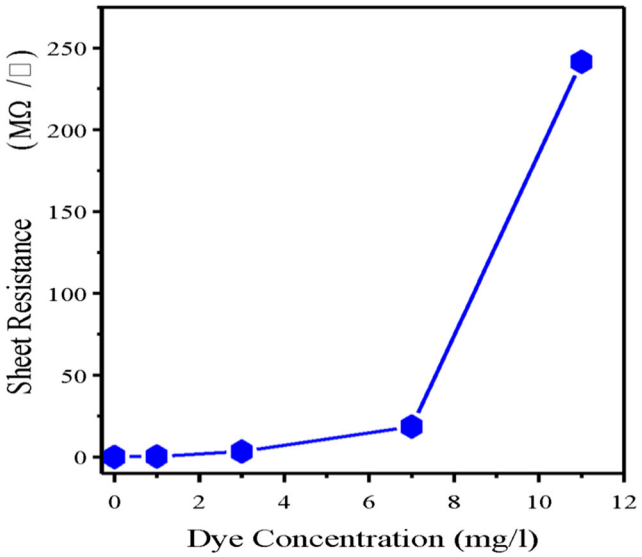

Fig. 8 Variation of sheet resistance of MB dye–interacted polyaniline with concentration of MB dye

crystalline polymer system, the hopping mechanism can play a significant contribution in electrical charge transport. In this work, the crystallinity of the polyaniline remains almost unaltered even after the MB dye interaction as observed from XRD results. Thus, the interaction of the polyaniline with dye mainly affects the intra-chain charge transport process. Furthermore, the intra-chain transport is much faster than the inter-chain one, and thus, a substantial effect can be observed in the electrical conductivity of polyaniline after MB dye interaction. The electrical conductivity variation of polyaniline with MB dye interaction is depicted in Fig. 6. It has been observed that the electrical conductivity is reduced significantly with increasing concentration of MB dye, indicating a convenient way of controlling the electrical conductivity and tuning it towards lower conductivity or higher resistivity.

The MB dye interaction brings an operative localization of the charge carriers bringing a control over the intra-chain carrier movement, thus increasing the resistivity. The mechanism of localization of polarons in the polymer backbone is based on

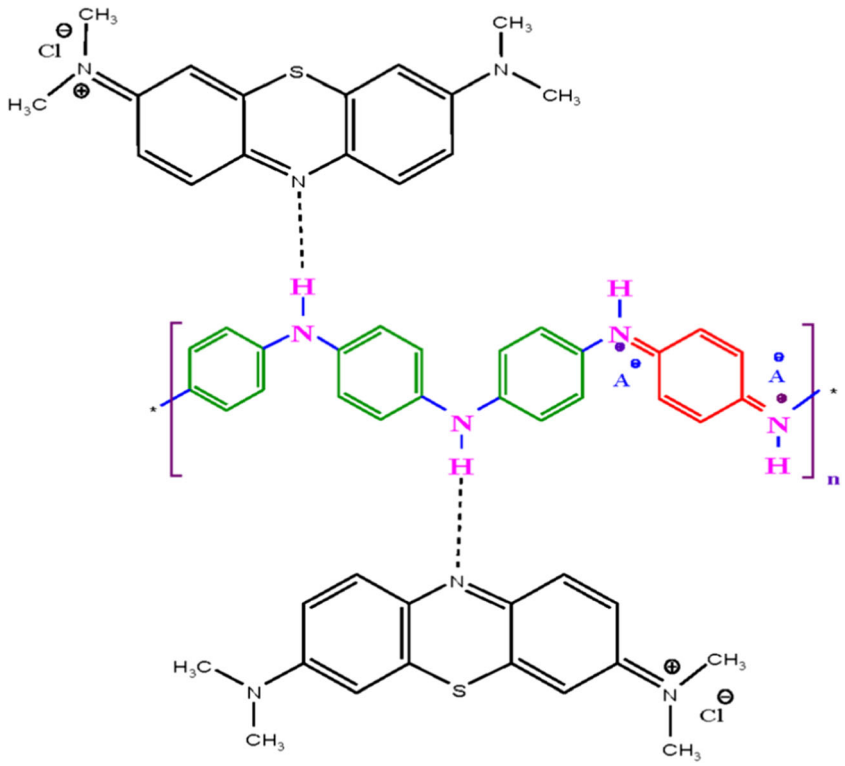

Fig. 7 Schematic representation of MB dye interaction with polyaniline

the interaction of the cationic MB dye with the polymer chain as illustrated in Fig. 7.

The delocalization of the electronic states relies on the resonance-stabilized structure of the polymer. Molecular arrangement must be conjugated and allow the charge defect states to propagate through the polymer chain for the charge transfer. The interaction of the MB dye with the polymer chain at first prevents the formation of polaron at the interaction site of the chain and thus reduces the number carrier. Secondly, it does not allow alteration of the σ and π bonds in the polymer backbone. As a result, the polyaniline interacted with the MB dye is not a good medium for the propagation of the charged defect states through its chain, affecting the intra-chain charge transport.

As a result, the resistivity increases, and the variation of sheet resistance of the polyaniline-implanted cellulose after MB dye interaction at different concentrations is depicted in Fig. 8. One can clearly observe a remarkable increase in sheet resistance with the increasing concentration of MB dye with an excellent tuning over a wide range.

Conclusions

Interaction of MB dye with polyaniline has been studied in this article with an objective to bring a control over the electrical transport properties of the polyaniline prepared on flexible cellulose sheet. MB dye mainly affects the intra-chain transport properties by localizing the polarons in the polymer backbone. The chemical attachment of MB dye with the polyaniline prevents the alteration of σ and π bonds in that part of the chain, and thus, the polaron already existing in the chain becomes localized. The electrical studies of the polyaniline interacted with MB dye on cellulose sheet show an excellent control of its electrical transport properties with a remarkable 10,000 times increase in sheet resistance. This wide-range control and tuning in its electrical transport have achieved keeping its optical band gap within the range of 2.47 to 2.63 eV, which lies on a suitable range of values for electronic and optoelectronic applications.

Acknowledgments The authors acknowledge the Department of Science and Technology, Government of India, for providing the UV-Vis-NIR measurement facility through the FIST project (SR/FST/PSI-196/2014). The authors acknowledge the Central Research Facility (CRF) of NIT Agartala for providing the XRD and SEM measurement facility.

Funding information This work is funded by the Council of Scientific and Industrial Research (CSIR), Government of India, sanction order reference no. 22/0744/17/EMR-II.

Compliance with ethical standards

Conflict of interest The authors declare that they have no conflict of interest.

References

1. Choi IY, Lee J, Ahn H, Lee J, Choi HC, Park MJ (2015) High-conductivity two-dimensional polyaniline nanosheets developed on ice surfaces. Angew Chem Int Ed 54:10497–10501
2. Mostafa NY, Mohamed MB, Imam NG, Alhamyani M, Heiba ZK (2016) Electrical and optical properties of hydrogen titanate nanotube/PANI hybrid nanocomposites. Colloid Polym Sci 294: 215–224
3. Sehgal P, Narula AK (2015) Structural, morphological, optical, and electrical transport studies of poly (3-methoxythiophene)/NiO hybrid nanocomposites. Colloid Polym Sci 293:2689–2699
4. Hajipour AR, Jajarmi S, Khorsandi Z (2017) Copper nanoparticles supported on polyaniline-functionalized multiwall carbon nanotubes: an efficient and recyclable catalyst for synthesis of unsymmetric sulfides using potassium ethyl xanthogenate in water. Appl Organomet Chem 31:e3697
5. Deb K, Bera A, Saha B (2016) Tuning of electrical and optical properties of polyaniline incorporated functional paper for flexible circuits through oxidative chemical polymerization. RSC Adv 6: 94795–94802
6. Tang L, Shim J-J (2013) Electrochemical property of graphene oxide/polyaniline composite prepared by in situ interfacial polymerization. Colloid Polym Sci 291:2237–2243
7. Liu T, Shao G, Ji M, Wang G (2015) Polyaniline/MnO_2 composite with high performance as supercapacitor electrode via pulse electrodeposition. Polym Compos 36:113–120
8. Pourjavadi A, Doroudian M, Moghanaki AA, Bennett C (2017) Magnetic GO-PANI decorated with Au NPs: a highly efficient and reusable catalyst for reduction of dyes and nitro aromatic compounds. Appl Organomet Chem 31:e3881
9. Hu W, Chen H, Li CM (2015) One-step synthesis of monodisperse gold dendrite@ polypyrrole core-shell nanoparticles and their enhanced catalytic durability. Colloid Polym Sci 293:505–512
10. Lay M, González I, Tarrés JA, Pellicer N, Bun KN, Vilaseca F (2017) High electrical and electrochemical properties in bacterial cellulose/polypyrrole membranes. Eur Polym J 91:1–9
11. Dai X, Li A, Wu F, Xie A (2016) Solid-state synthesis of a conducting polythiophene as efficient Pt-free thin film counter electrode for dye-sensitized solar cells. Mater Lett 174:91–94
12. Mohsennia M, Bidgoli MM, Boroumand FA, Nia AM (2015) Electrically conductive polyaniline as hole-injection layer for MEH-PPV: BT based polymer light emitting diodes. Mater Sci Eng B 197:25–30
13. Kim YH, Han TH, Cho H, Min SY, Lee CL, Lee TW (2014) Polyethylene imine as an ideal interlayer for highly efficient inverted polymer light-emitting diodes. Adv Funct Mater 24: 3808–3381
14. Hu Z, Zhang K, Huang F, Cao Y (2015) Water/alcohol soluble conjugated polymers for the interface engineering of highly efficient polymer light-emitting diodes and polymer solar cells. Chem Commun 51:5572–5585
15. Gao M, Xu Y, Bai Y, Jin S (2014) Effect of electro-polymerization time on the performance of poly (3, 4-ethylenedioxythiophene) counter electrode for dye-sensitized solar cells. Appl Surf Sci 289: 145–149
16. Cindrella L (2016) CuO-PANI nanostructure with tunable spectral selectivity for solar selective coating application. Appl Surf Sci 378: 245–252
17. Wan L, Wang B, Wang S, Wang X, Guo Z, Xiong H, Dong B (2014) Water-soluble polyaniline/graphene prepared by in situ polymerization in graphene dispersions and use as counter-electrode materials for dye-sensitized solar cells. React Func Polym 79:47–53

18. Shinde SS, Gund GS, Kumbhar VS, Patil BH, Lokhande CD (2013) Novel chemical synthesis of polypyrrole thin film electrodes for supercapacitor application. Eur Polym J 49:3734–3739
19. Chang X, Hu R, Sun S, Liu J, Lei Y, Liu T, Dong L, Yin Y (2018) Sunlight-charged electrochromic battery based on hybrid film of tungsten oxide and polyaniline. Appl Surf Sci 441:105–112
20. Hu Z, Zu L, Jiang Y, Lian H, Liu Y, Wang X, Cui X (2015) High performance nanocomposite electrodes of mesoporous silica platelet-polyaniline synthesized via impregnation polymerization. Polym Compos 38:1616–1623
21. Taher A, Choudhary M, Nandi D, Siwal S, Mallick K (2018) Polymer-supported palladium: a hybrid system for multifunctional catalytic application. Appl Organomet Chem 32:e3898
22. Chen J, Zhang J, Zhu D, Li T (2018) Porphyrin-based polymer-supported palladium as an excellent and recyclable catalyst for Suzuki–Miyaura coupling reaction in water. Appl Organomet Chem 32:e3996
23. Agrawal A, Satapathy A (2015) Effect of Al_2O_3 addition on thermo-electrical properties of polymer composites: an experimental investigation. Polym Compos 36:102–112
24. Wu J, Sun Y, Pei WB, Huang L, Xu W, Zhang Q (2014) Polypyrrole nanotube film for flexible thermoelectric application. Synth Met 196:173–177
25. Lai C, Li J, Xiang X, Wang L, Liu D (2018) Effects of side groups on the thermoelectric properties of composites based on conjugated poly (3, 4-ethylenedioxythiophene methine)s with low bandgaps. Polym Compos 39:126–134
26. He X, Liu G, Yan B, Suo H, Zhao C (2016) Significant enhancement of electrochemical behaviour by incorporation of carboxyl group functionalized carbon nanotubes into polyaniline based supercapacitor. Eur Polym J 83:53–59
27. Gui D, Liu C, Chen F, Liu J (2014) Preparation of polyaniline/graphene oxide nanocomposite for the application of supercapacitor. Appl Surf Sci 307:172–177
28. Wu T, Wang C, Mo Y, Wang X, Fan J, Xu Q, Min Y (2017) A ternary composite with manganese dioxide nanorods and graphene nanoribbons embedded in a polyaniline matrix for high-performance supercapacitors. RSC Adv 7:33591
29. Gholami M, Nia PM, Narimani L, Sokhakian M, Alias Y (2016) Flexible supercapacitor based on electrochemically synthesized pyrrole formyl pyrrole copolymer coated on carbon microfibers. Appl Surf Sci 378:259–269
30. Kumar R, Yadav BC (2016) Fabrication of polyaniline (PANI)—tungsten oxide (WO_3) composite for humidity sensing application. J Inorg Organomet Polym Mater 26:1421–1427
31. Nia PM, Lorestani F, Meng WP, Alias Y (2015) A novel non-enzymatic H_2O_2 sensor based on polypyrrole nanofibers–silver nanoparticles decorated reduced graphene oxide nano composites. Appl Surf Sci 332:648–656
32. Sultan A, Ahmad S, Mohammad F (2017) Synthesis, characterization and electrical properties of polypyrrole/zirconia nanocomposite and its application as ethene gas sensor. Polym Polym Compos 25: 695–704
33. Patil UV, Ramgir NS, Karmakar N, Bhogale A, Debnath AK, Aswal DK, Gupta SK, Kothari DC (2015) Room temperature ammonia sensor based on copper nanoparticle intercalated polyaniline nanocomposite thin films. Appl Surf Sci 339:69–74
34. Mitra M, Ghosh A, Mondal A, Kargupta K, Ganguly S, Banerjee D (2017) Facile synthesis of aluminium doped zinc oxide-polyaniline hybrids for photoluminescence and enhanced visible-light assisted photo-degradation of organic contaminants. Appl Surf Sci 402: 418–428
35. Yu P, Zhao X, Li Y, Zhang Q (2017) Controllable growth of polyaniline nanowire arrays on hierarchical macro/mesoporous graphene foams for high-performance flexible supercapacitors. Appl Surf Sci 393:37–45
36. Wang L, Sun S, He Y, He N, Zhang F, Yao Y, Zhang B, Zhuang X, Chen Y (2018) Viologen-bridged polyaniline based multifunctional heterofilms for all-solid-state supercapacitors and memory devices. Eur Polym J 98:125–136
37. Hajibadali A, Nejad MB, Farzi G (2015) Schottky diodes based on polyaniline/multi-walled carbon nanotube composites. Braz J Phys 45:394–398
38. Ghushe JM, Giripunje SM, Kondawar SB (2016) Effect of metal doped zinc oxide nanorods on photoelectrical characteristics of ZnO/polyaniline heterojunction. J Inorg Organomet Polym Mater 26:370–375
39. Quan L, Sun J, Bai S, Luo R, Li D, Chen A, Liu CC (2017) A flexible sensor based on polyaniline hybrid using ZnO as template and sensing properties to triethylamine at room temperature. Appl Surf Sci 399:583–591
40. Bora C, Kalita A, Das D, Dolui SK, Mukhopadhyay PK (2014) Preparation of polyaniline/nickel oxide nanocomposites by liquid/liquid interfacial polymerization and evaluation of their electrical, electrochemical and magnetic properties. Polym Int 63:445–452
41. Khan MMR, Wee YK, Mahmood WAK (2015) Synthesis of PANI-CaO composite nanofibers with controllable diameter and electrical conductivity. Polym Compos 36:359–366
42. Sabu NA, Francis X, Anjaly J, Sankararaman S, Varghese T (2017) Enhanced structural and optical properties of the polyaniline-calcium tungstate (PANI-$CaWO_4$) nanocomposite for electronics applications. Eur Phys J Plus 132:290
43. Goswami M, Ghosh R, Maruyama T, Meikap AK (2016) Polyaniline/carbon nanotube/CdS quantum dot composites with enhanced optical and electrical properties. Appl Surf Sci 364: 176–180
44. Zhang W, Guo H, Sun H, Zeng R (2017) Constructing ternary polyaniline-graphene-TiO_2 hybrids with enhanced photoelectrochemical performance in photo-generated cathodic protection. Appl Surf Sci 410:547–556
45. Vempati S, Ertas Y, Babu VJ, Uyar T (2016) Optoelectronic properties of layered titanate nanostructure and polyaniline impregnated devices. ChemistrySelect 1:5885–5891
46. De Barros RA, De Azevedo WM, De Aguiar FM (2003) Photo-induced polymerization of polyaniline. Mater Charac 50:131–134
47. Janaky C, De Tacconi NR, Chanmanee W, Rajeshwar K (2012) Bringing conjugated polymers and oxide nanoarchitectures into intimate contact: light-induced electrodeposition of polypyrrole and polyaniline on nanoporous WO_3 or TiO_2 nanotube array. J Phys Chem C 116:19145–19155
48. Oueiny C, Berlioz S, Perrin FX (2016) Assembly of polyaniline nanotubes by interfacial polymerization for corrosion protection. Phys Chem Chem Phys 18:3504–3509
49. Bogdanovic U, Pasti IA, Marjanovic GC, Mitric M, Ahrenkiel SP, Vodnik VV (2015) Interfacial synthesis of gold–polyaniline nanocomposite and its electrocatalytic application. ACS Appl Mater Interfaces 7:28393–28403
50. Guo Y, Zhou Y (2007) Polyaniline nanofibers fabricated by electrochemical polymerization: a mechanistic study. Eur Polym J 43: 2292–2297
51. Arjomandi J, Tadayyonfar S (2014) Electrochemical synthesis and in situ spectroelectrochemistry of conducting polymer nanocomposites. I. Polyaniline/TiO_2, polyaniline/ZnO, and polyaniline/TiO_2+ ZnO. Polym Compos 35:351–363
52. Xu H, Zhang J, Chen Y, Lu H, Zhuang J (2014) Electrochemical polymerization of polyaniline doped with Cu^{2+} as the electrode material for electrochemical supercapacitors. RSC Adv 4:5547–5552
53. Cho S, Shin KH, Jang J (2013) Enhanced electrochemical performance of highly porous supercapacitor electrodes based on solution processed polyaniline thin films. ACS Appl Mater Interfaces 5: 9186–9193

54. Kim BJ, Oh SG, Han MG, Im SS (2000) Preparation of polyaniline nanoparticles in micellar solutions as polymerization medium. Langmuir 16:5841–5845
55. Karagoz B, Sirkecioglu O, Bicak N (2013) Surface rejuvenation for multilayer metal deposition on polymer microspheres via self-seeded electroless plating. Appl Surf Sci 285:395–402
56. Li Y, Yu Y, Wu L, Zhi J (2013) Processable polyaniline/titania nanocomposites with good photocatalytic and conductivity properties prepared via peroxo-titanium complex catalyzed emulsion polymerization approach. Appl Surf Sci 273:135–143
57. Kim JY, Lee JH, Kwon SJ (2007) The manufacture and properties of polyaniline nano-films prepared through vapor-phase polymerization. Synth Met 157:336–342
58. Jun TS, Kim CK, Kim YS (2014) Vapor phase polymerization of polyaniline nanotubes using Mn_3O_4 nanofibers as an oxidant. Mater Lett 133:17–19
59. Jatratkar AA, Yadav JB, Deshmukh RR, Barshilia HC, Puri V, Puri RK (2016) Impact of low-pressure glow-discharge-pulsed plasma polymerization on properties of polyaniline thin films. Phys Scr 91:125501
60. Pal AR, Sarma BK, Adhikary NC, Chutia J, Bailung H (2011) TiO_2/polyaniline nanocomposite films prepared by magnetron sputtering combined with plasma polymerization process. Appl Surf Sci 258:1199–1205
61. Bhanvase BA, Sonawane SH (2017) Sonochemical preparation of hybrid polymer nanocomposites: properties and applications. Hybrid Polym Compos Mater 4:321–342
62. Wang Y, Bian L, Tan D, Chen S, Gan Y (2017) Sonochemical synthesis of "sea-island" structure silver/polyaniline nanocomposites for the detection of l-tyrosine. J Thermoplast Compos Mater 30: 1033–1044
63. Bhowmik KL, Deb K, Bera A, Nath RK, Saha B (2016) Charge transport through polyaniline incorporated electrically conducting functional paper. J Phys Chem C 120:5855–5860
64. Wang H, Hao Q, Yang X, Lu L, Wang X (2010) Effect of graphene oxide on the properties of its composite with polyaniline. ACS Appl Mater Interfaces 2:821–828
65. Patil RB, Jatratkar AA, Devan RS, Ma YR, Puri RK, Puri V, Yadav JB (2015) Effect of pH on the properties of chemical bath deposited polyaniline thin film. Appl Surf Sci 327:201–204
66. Abdiryim T, Xiao-Gang Z, Jamal R (2005) Comparative studies of solid-state synthesized polyaniline doped with inorganic acids. Mater Chem Phys 90:367–372
67. Xue M, Zou M, Zhao J, Zhanab Z, Zhao S (2015) Green preparation of fluorescent carbon dots from lychee seeds and their application for the selective detection of methylene blue and imaging in living cells. J Mater Chem B 3:6783–6789
68. Lei T, Wang JY, Pei J (2014) Design, synthesis, and structure−property relationships of isoindigo-based conjugated polymers. Acc Chem Res 47:1117–1126